ACS SENSORS

Article

Cite This: ACS Sens. 2019, 4, 2802−2808

pubs.acs.org/acssensors

A Dual-Sensing DNA Nanostructure with an Ultrabroad Detection Range

Byunghwa Kang,[†] Soyeon V. Park,[†] Hyongsok Tom Soh,*[,§] and Seung Soo Oh*[,†,‡]

[†]Department of Materials Science and Engineering and [‡]School of Interdisciplinary Bioscience and Bioengineering, Pohang University of Science and Technology (POSTECH), 77 Cheongam-Ro, Nam-Gu, Pohang 37673, Gyeongbuk, South Korea

[§]Department of Electrical Engineering and Department of Radiology, Canary Center at Stanford University, 3155 Porter Drive, Stanford, California 94305, United States

Supporting Information

ABSTRACT: Despite considerable interest in the development of biosensors that can measure analyte concentrations with a dynamic range spanning many orders of magnitude, this goal has proven difficult to achieve. We describe here a modular biosensor architecture that integrates two different readout mechanisms into a single-molecule construct that can achieve target detection across an extraordinarily broad dynamic range. Our dual-mode readout DNA biosensor combines an aptamer and a DNAzyme to quantify adenosine triphosphate (ATP) with two different mechanisms, which respond to low (micromolar) and high (millimolar) concentrations by generating distinct readouts based on changes in fluorescence and absorbance, respectively. Importantly, we have also devised regulatory strategies to fine-tune the target detection range of each sensor module by controlling the target-sensitivity of each readout mechanism. Using this strategy, we report the detection of ATP at a dynamic range spanning 1−500 000 μM, more than 5 orders of magnitude, representing the largest dynamic range reported to date with a single biosensor construct.

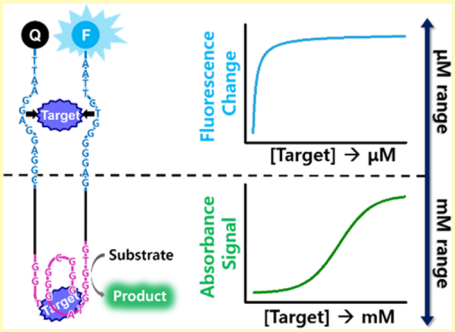

KEYWORDS: *ATP, aptamer, DNAzyme, peroxidation, modular structure, dual-mode readout*

In nature, many biological receptors have evolved the capacity to respond to ligands across a broad dynamic range of concentrations.[1,2] This is important, as their cognate molecular targets, such as hormones, metal ions, and viruses, may be present across a broad spectrum of concentrations.[3−5] For instance, the JAK2/STAT5 signaling pathway, which is involved in cell differentiation and survival, is capable of responding to a 1000-fold change in the concentration of the hormone erythropoietin (Epo).[6] This pathway achieves the broad dynamic range for Epo response through the combined action of two regulatory mechanisms, governed by CIS and SOCS3.[6] In this signaling pathway, binding of Epo to its receptor induces JAK2 phosphorylation, followed by the activation of the transcription factor STAT5; STAT5 subsequently binds to the Epo receptor to generate a signaling output.[7] At low levels of Epo (10^{-9} U/cell), CIS acts as a physical competitor that blocks STAT5 binding to the Epo receptor; at higher Epo levels (10^{-6} U/cell), SOCS3 acts as a catalytic inhibitor for Epo-induced JAK2 phosphorylation. The combined action of these two regulators enables cells to respond to changes in Epo concentrations spanning a 1000-fold range.

Unfortunately, most synthetic biosensors have a much narrower detection range. For example, typical biosensors based on affinity reagents such as antibodies rely on Langmuir binding physics to detect targets, such that their dynamic ranges are both inherently narrow (i.e., typically on the order of 81-fold) and extremely difficult to shift.[8,9] Enzyme-based detection systems likewise have narrowly defined detection ranges because of intrinsic features of the enzyme in question, limiting control over the sensor dynamic range.[10] These fundamental limitations make it difficult to cope with wide variations in target concentration.[11,12] Many researchers have proposed ideas to extend the dynamic range of biosensors. For example, Ricci et al. have designed diverse DNA-based sensors that can achieve target detection across 3 orders of magnitude by making use of mutation- or allosteric regulation-based approaches.[13−16] However, even broader detection ranges are needed for many clinically relevant biological targets; for example, the physiological concentrations of HIV and prostate-specific antigen can vary over more than 4 orders of magnitude.[5,17,18] Therefore, there remains a strong need for novel strategies for the development of simple molecular biosensors with ultra-broad detection ranges.

We present here a novel biosensor design that couples together two DNA-based modules with distinct sensing modalities, enabling a semiquantitative target detection over a concentration range spanning more than 5 orders of magnitude. Our "dual-mode readout DNA" (DMRD) nanostructure is capable of detecting adenosine triphosphate

Received: August 6, 2019
Accepted: September 24, 2019
Published: September 24, 2019

DOI: 10.1021/acssensors.9b01503
ACS Sens. 2019, 4, 2802−2808

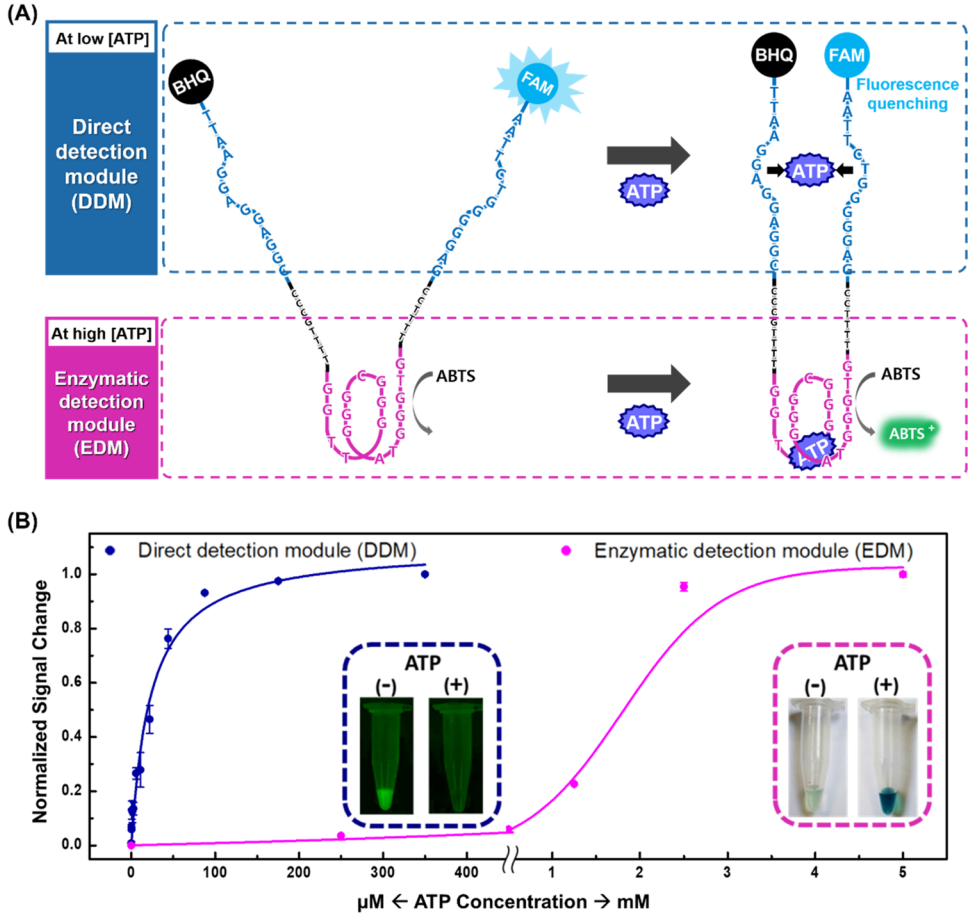

Figure 1. Modular ATP-sensing platform that can achieve a broad dynamic range of detection. (A) Our dual-mode readout DNA (DMRD) nanostructure contains two distinct ATP-sensing modules. The direct detection module (DDM) uses a split ATP-binding aptamer (top), where target binding induces an aptamer assembly and thereby brings coupled fluorophore and quencher groups into close proximity. This leads to a measurable decrease in FAM signal that correlates with ATP levels at relatively low (micromolar) concentrations. The enzymatic detection module (EDM) comprises an ATP-enhanced DNAzyme that uses ATP as a cofactor (bottom) that increases its catalytic activity, leading to increased oxidation of ABTS. The accumulation of $ABTS^+$ can be measured by a change in absorbance, enabling detection of ATP at higher (millimolar) concentrations. (B) Target detection with the DMRD. The DDM detects ATP in the micromolar concentration range (blue line), and we can observe the ATP-induced decrease in FAM fluorescence at 535 nm (blue inset). The peroxidase activity of the EDM is accelerated by the presence of ATP at millimolar concentrations (magenta line), and $ABTS^+$ accumulation leads to increased absorbance at 418 nm that can be observed by naked eye (magenta inset).

(ATP) at two different concentration ranges with two different readouts: fluorescence and absorbance. Moreover, the target detection range of the DMRD is highly tunable, and we have developed strategies for refining the sensitivity of both modules to shape the concentration range at which the sensor produces a response. Using this tuning approach, we demonstrate that our DMRD can successfully report ATP concentrations ranging from 1 μM to 500 mM, a dynamic range spanning a 500 000-fold concentration difference that is presently impossible to obtain with either sensing mechanism alone and represents the widest target detection range reported to date for a single DNA-based biosensor construct.[13]

RESULTS AND DISCUSSION

Modular Design of the DMRD. As a demonstration of our DMRD concept, we developed a modular ATP sensor (Figure 1A). The DMRD comprises two different sensing modules: a direct detection module (DDM) and an enzymatic detection module (EDM). The DDM (Figure 1A, top) is an adaptation of a previously published ATP aptamer, which has been engineered to fluoresce in a concentration-dependent manner.[19] The DDM consists of two single-stranded DNA fragments that have been respectively labeled with fluorescein (FAM) and Black Hole Quencher 1 (BHQ1). These strands remain separated in the absence of ATP, generating an unquenched fluorescent signal. When ATP is added, these two fragments undergo binding-induced assembly that brings FAM and BHQ1 into close proximity, leading to a decrease of fluorescent signal at 535 nm. This aptamer-based DDM is designed to detect relatively low ATP concentrations ($\geq$1 μM).

The two fragments of the DDM are in turn linked to the ends of the EDM, which provides the second readout mechanism (Figure 1A, bottom). The EDM incorporates a DNAzyme, which folds into a G-quadruplex structure that forms a complex with hemin.[20] This DNAzyme/hemin complex exhibits modest peroxidase activity, but this catalytic activity is greatly enhanced by the presence of ATP.[21,22] Such ATP-assisted peroxidation can cause rapid oxidation of substrates such as 2,2′-azino-bis(3-ethylbenzothiazoline-6-sulfonic acid) (ABTS), leading to accumulation of the product $ABTS^+$. This $ABTS^+$ accumulation produces a proportional

DOI: 10.1021/acssensors.9b01503
ACS Sens. 2019, 4, 2802−2808

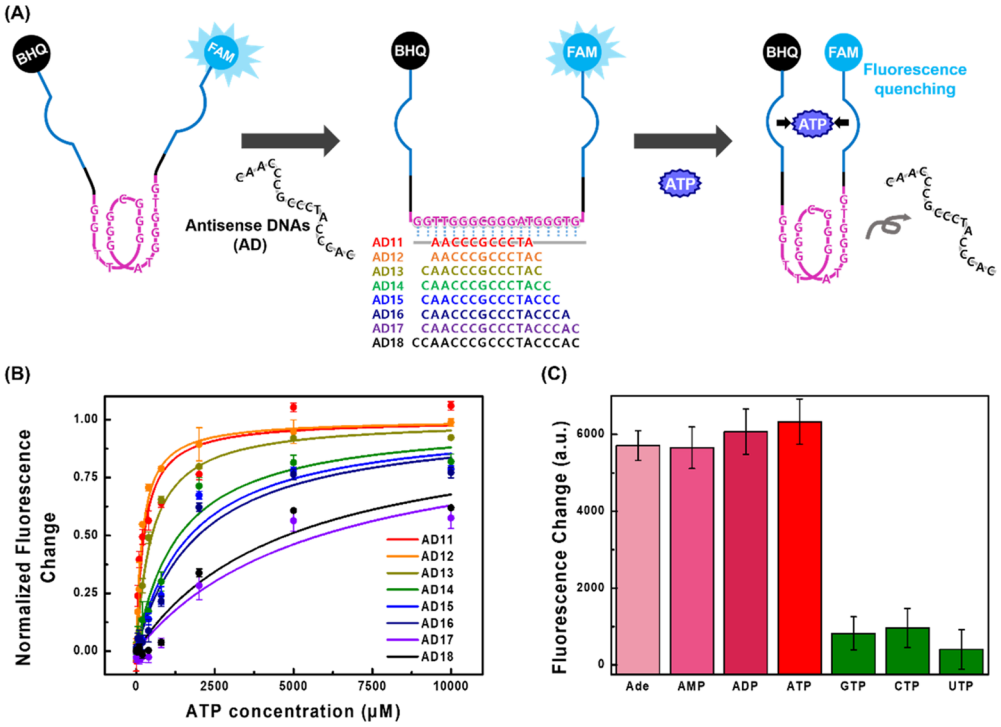

Figure 2. Tuning the ATP response of the DDM with antisense DNAs. (A) Target detection range of the DDM can be fine-tuned with antisense DNA strands that hybridize with the EDM. This hybridization hinders target-induced structure switching, requiring higher ATP concentrations to generate fluorescence quenching. (B) Antisense strands with lengths ranging from 11 to 18 nt (AD11 to AD18) differentially affected the ATP response of this module, yielding DDMs that can cover a broader ATP detection range from 1 to 7500 μM. (C) DDM target specificity in the presence of AD11. All ATP analogues were present at 1 mM. Guanosine triphosphate (GTP), cytidine triphosphate (CTP), and uridine triphosphate (UTP) failed to yield strong signal, whereas adenosine (Ade) and its derivatives (ATP, adenosine diphosphate (ADP), and adenosine monophosphate (AMP)) produced a similar fluorescence change.

absorbance change at 418 nm,[23] generating a colorimetric signal that can be detected by the naked eye at high ATP concentrations (>1 mM).

These two modules can thus be combined to measure the presence of ATP at very different concentration ranges (Figure 1B). The DDM, which has a dissociation constant (K_d) of 23.1 μM, has the capacity to report ATP concentrations in the range of ~1−100 μM based on fluorescence measurements. On the other hand, the EDM exhibits target-assisted peroxidase activity in a millimolar concentration range spanning roughly 0.74−2.92 mM, with the ATP-dependent absorbance change producing a strong green color that is even detectable by naked eye. DDM sensing has no impact on the peroxidase activity of the EDM, which only produces a response at millimolar ATP concentrations at which the DDM's fluorescent signal has already become saturated. As a consequence, our modular DMRD design can cover a broad dynamic range for target detection through its dual-readout system.

Optimizing DDM Performance. The detection range of the DDM can be fine-tuned through the use of antisense DNAs that modulate aptamer−target binding (Figure 2A), yielding the capacity to discriminate ATP concentrations ranging from 1 μM to 7.5 mM. These antisense sequences (Table S1) are complementary to the central domain of our DMRD, which also comprises the EDM. Hybridization of the antisense DNA to the DMRD hinders ATP-induced structure switching of the aptamer by increasing separation between the two segments of the DDM. As a consequence, higher concentrations of ATP must be present to outcompete the effect of the antisense DNA, thereby shifting the dynamic range of the DDM for ATP detection.

One can precisely tune the target detection range of the DDM by changing the length of the antisense DNA (Figure 2B). For example, a 13-nt antisense DNA produced a sensor with a half-maximal effective concentration (EC_{50}) of 494 μM (Table S2), while the DDM without the antisense DNA yields an EC_{50} of 23.1 μM. As a result, the original target detection range of the DDM (1−100 μM) can be shifted to 57.2−2998 μM (Table S3). With a shorter, 11-nt antisense DNA, we can lower this EC_{50} to 238 μM, achieving a detection range of 33.9−1782 μM. In contrast, a much longer antisense strand (18 nt) produced a >20-fold greater EC_{50} value of 4768 μM, such that our DDM can respond to a range of ATP concentrations from 346.8 to 7440 μM.

As expected, the relationship between the length of the antisense DNA and the resulting EC_{50} value follows an Arrhenius plot (Figure S1). This is because the main interactions expected from our DDM, between the DMRD and the antisense DNA and between the aptamer and ATP, are based on Gibbs free energy change (ΔG). From the extrapolation of our Arrhenius plot, we calculated the EC_{50} value for the antisense-free DDM, which is equivalent to the K_d of the ATP-binding aptamer (19.98 μM). Microscale thermophoresis measurements confirmed our calculations of the inherent binding affinity of the aptamer, yielding a K_d value of 23.1 μM based on Langmuirian binding between the target and the aptamer (Figure S2). The hybridization of antisense DNA interferes with the DDM's structure-switching, allowing the binding behavior of the DDM to follow our hybridization

DOI: 10.1021/acssensors.9b01503
ACS Sens. 2019, 4, 2802−2808

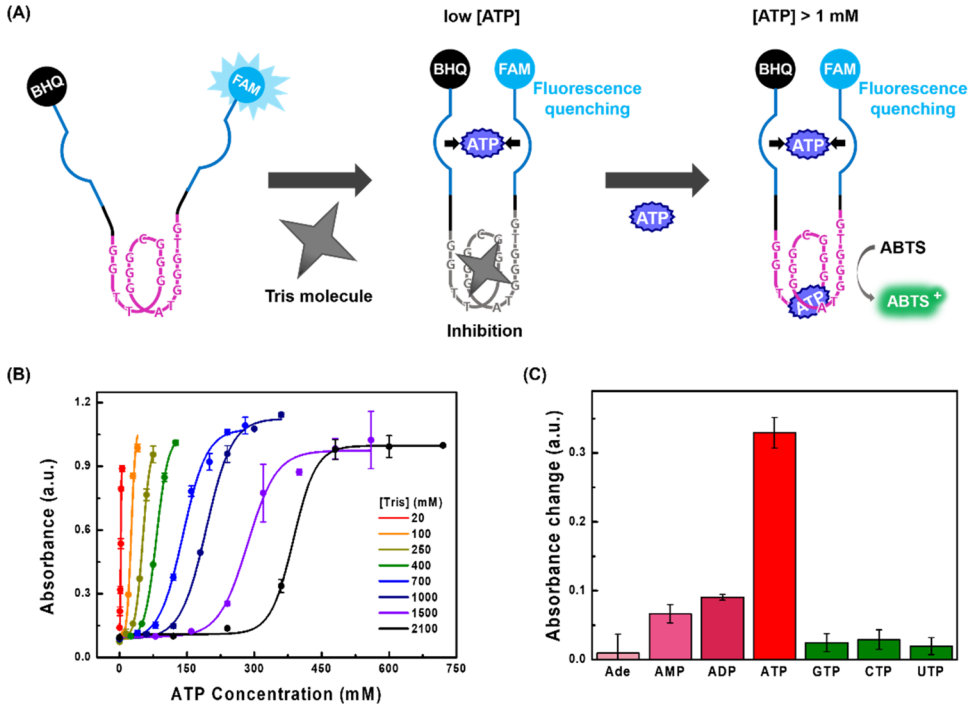

Figure 3. EDM responds to ATP at millimolar concentrations, with a dynamic range that can be tuned by the presence of Tris. (A) Tris acts as a catalytic inhibitor of the EDM at low or moderate ATP concentrations, requiring more ATP to restore the reduced catalytic activity. (B) We obtained different calibration curves for ATP detection at different concentrations of Tris, where the ATP concentration required to generate a readout increased in proportion to the Tris concentration. With this tuning strategy, the EDM can achieve ATP detection at a range of ~1−500 mM. Each peroxidation reaction was performed at room temperature for 1 h. (C) Target specificity of our EDM in 20 mM Tris, with 3 mM of various ATP analogues. Adenosine, GTP, CTP, and UTP failed to generate a readout; ATP showed very strong catalytic enhancement, while ADP and AMP exhibited a much weaker activity.

energy-based Arrhenius plot, so that the DDM paired with an antisense strand exhibits a much higher EC_{50} than the K_d of the antisense-free DDM. Thus, DDM constructs coupled with varying lengths of antisense DNA can achieve finely tuned binding curves that enable an ATP detection range spanning 1−7500 μM (Figure 2B).

Our DDM consistently remained highly specific for ATP and other adenosine-derived molecules, without responding to other analytes with chemically similar structures (Figures 2C and S3). For example, when the DDM was hybridized with the 11-nt antisense strand (AD11), it produced a similar reduction in fluorescence signal in response to adenosine, ATP, ADP, and AMP, but other nucleoside derivatives such as GTP, CTP, and UTP generated minimal signal change (Figure 2C). Importantly, this target specificity of the DDM does not differ in the absence of antisense strand (Figure S3), indicating that the antisense strand does not alter the nucleobase-specificity of the DDM. We therefore conclude that the presence of the antisense DNA only affects the thermodynamics of ATP binding, and thus the module's target sensitivity and detection range.

Optimizing EDM Performance. We were likewise able to tune the responsiveness of the EDM by modulating the chemical conditions of the assay, which enabled us to achieve a dynamic range spanning roughly 1−500 mM with the same construct. Tris(hydroxymethyl)aminomethane (Tris) binds antagonistically to the EDM, thereby decreasing its catalytic activity, and can thus be used to shift its target detection range (Figure 3A). This Tris-dependent catalytic inhibition is a new finding, and the underlying mechanism may be related to a previous report that Tris can trap intermediate radicals (·OH) and thereby block the peroxidation of cellular lipids.[24,25] In the absence of Tris, the catalytic activity of the EDM is dramatically enhanced by the presence of ATP, which serves as a cofactor for the DNAzyme-catalyzed peroxidase reaction. The presence of Tris molecules has an inhibitory effect and reduces the rate of this reaction, such that a higher concentration of ATP is needed to restore the DNAzyme's peroxidase activity and thus generate an absorbance signal.

We experimentally confirmed our ability to fine-tune the dynamic range of the EDM by adjusting the concentration of Tris from 20 mM to 2.1 M, obtaining eight different calibration curves for ATP detection (Figure 3B). At the lowest Tris concentration (20 mM), the EDM remained sensitive to relatively low ATP concentrations, ranging from 1.36 to 4.19 mM. At an intermediate concentration (700 mM Tris), the EDM was responsive to ATP concentrations ranging from 88.6 to 198 mM. Very high Tris concentrations greatly reduced this module's sensitivity, and at 2.1 M Tris, the EDM exhibited a dynamic range that spanned submolar concentrations (282−506 mM). Thus, manipulating the chemical environment in this fashion can extend the ATP detection range achieved by the EDM from as low as 0.74 mM to as high as 506 mM.

Like the original DNAzyme,[22] our EDM retains excellent specificity for ATP in the presence of Tris and can even distinguish between ATP and other adenosine-based compounds (Figure 3C). ATP analogues such as GTP, CTP, and UTP failed to generate an enhanced absorbance readout from the EDM in the presence of 20 mM Tris. ADP and AMP produced a much weaker response, while adenosine itself showed negligible influence on the peroxidation reaction. We identified the same ATP specificity in experiments without Tris

DOI: 10.1021/acssensors.9b01503
ACS Sens. 2019, 4, 2802−2808

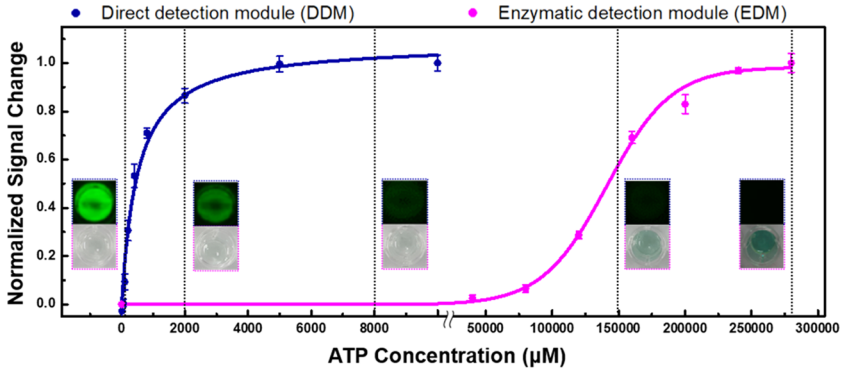

Figure 4. Applying the DMRD for ATP detection in different target concentration ranges. The concentration of ATP in an unknown sample can be represented by our dual-readout (fluorescence and absorbance) platform in a 96-well microplate, where each well contains a different length of antisense DNA or Tris concentration.

(Figure S4), indicating that the addition of Tris does not affect the ATP specificity of the DNAzyme. Moreover, our observations indicate that unlike the DDM, our EDM can discriminate ATP from other adenosine-containing molecules based on the number of phosphate groups, and thus exhibits superior specificity compared to the DDM. This is because ATP plays a very specific role as a cofactor in the peroxidase activity of the EDM, where it activates H_2O_2 and provides the energy for electron transfer,[26] whereas ATP binds to the DDM purely on the basis of intermolecular interactions. We found that the ATP specificity of DMRD is determined by the inherent discriminatory ability of each module, and our tuning strategy did not affect the specificity. Due to the intrinsic limitations of the aptamer used here, for instance, it is possible that one might encounter complications in reporting micromolar ATP concentrations in a sample containing various adenosine analogues, but our DMRD is still useful in that it can discriminate ATP from all other nucleoside triphosphates within its detection range. Alternative ATP aptamers[27−29] that can distinguish phosphate groups are available, and we note that their use in the DMRD has the potential to greatly improve ATP specificity even at micromolar ranges.

Dual Readouts for Ultrabroad Detection Range. We have demonstrated that these two modules, combined with the respective tuning mechanisms described above, enable the DMRD sensor to achieve an exceptionally broad dynamic range for ATP detection, from 1 μM to 500 mM, spanning more than 5 orders of magnitude. Consequently, we can quantitatively determine the ATP concentration in a sample through the combination of this dual-readout system with varying lengths of antisense strands or concentrations of Tris. If the unknown sample has an ATP concentration within the detection range of a particular experimental condition with DMRD, its concentration can be represented by the resulting specific fluorescence and absorbance intensities. As a demonstration, we added samples containing five different concentrations of ATP (200 μM, 2 mM, 8 mM, 150 mM, and 300 mM) to microplate wells containing the DMRD with AD13 and 700 mM Tris and observed both fluorescence and absorbance signals from each well (Figure 4). Likewise, we successfully measured ATP concentrations across 5 orders of magnitude (1 μM to 100 mM) using our DMRD in just two assay conditions (Table S5): 20 mM Tris without antisense strands and AD11 plus 400 mM Tris. These results show that a single assay condition can cover 3 orders of magnitude in concentration, and that detection of ATP across 5 orders of magnitude only requires two assay conditions. To achieve the same detection results as DMRD using the aptamer and DNAzyme separately, one would need to set up at least four experimental conditions.

CONCLUSIONS

In this work, we integrated two different ATP-sensing modules in a single DNA molecule, which we have termed the DMRD, to achieve an extremely broad target detection range. The DDM employs a split aptamer coupled with a fluorophore/quencher pair to produce a binding-induced fluorescence change at micromolar ATP concentrations, where the dynamic range can be modulated through the introduction of complementary antisense strands of varying lengths. In parallel, the EDM incorporates a DNAzyme that employs ATP as a cofactor, generating an absorbance change at millimolar ATP concentrations, and the dynamic range of this module can be further tuned by manipulating the concentration of Tris in the reaction mixture. By integrating these two sensing modules, our in vitro ATP-sensing platform can achieve ATP detection at concentrations ranging from 1 μM to 500 mM. This spans a 500 000-fold concentration difference, which represents the widest sensing range achieved by a single DNA-based biosensor.

It is important to note that we do not have to generate variants of the bioreceptor with different detection ranges through complicated processes such as mutational screening. In addition, we can make use of alternate signaling modalities in our DMRD construct by substituting FAM or ABTS with different signaling substrates. For instance, if we swap ABTS with luminol, the DMRD can be converted to a two-color fluorescence signaling system. Additionally, this integrated DMRD sensor design could conceivably be used to detect target molecules at localized sites in biological experiments. Local target detection, for example, at a cell surface or within an endosome, requires all necessary target-sensing elements to coexist in the same area, and our integrated sensing platform could enable accurate target detection under such conditions.[30]

We have demonstrated here the use of two different detection mechanisms in a monolithic biosensor construct to achieve an extremely wide range of target detection. To date, a variety of split aptamers[31−34] capable of recognizing targets including proteins (e.g., thrombin and protein tyrosine kinase-7 receptor) and small molecules (e.g., β-estradiol, deoxycholate, dehydroisoandrosterone-3-sulfate, deoxycorticosterone 21-glucoside, and cocaine) have been reported, along

DOI: 10.1021/acssensors.9b01503
ACS Sens. 2019, 4, 2802−2808

with several methodologies for engineering such constructs for new targets. Likewise, several nucleozymes[35−38] have been described whose activities are controlled by diverse catalytic activators or inhibitors (e.g., metal ions, amino acids, ethanol, and ascorbic acid), and these can also be applied to our modular system. More generally, the extension of our current modular approach to new targets is primarily limited by the availability of nucleozymes, but we believe that ongoing advancements in nucleic acid library screening techniques[39−44] will allow accelerated discovery of aptamers and nucleozymes, making our strategy suitable for use with many other molecular targets.

■ ASSOCIATED CONTENT

Supporting Information

The Supporting Information is available free of charge on the ACS Publications website at DOI: 10.1021/acssensors.9b01503.

DNA sequences; ATP detection range; EC_{50} values; Arrhenius plot; antisense-free target specificity; Tris-free target specificity; detection of ATP targets (PDF)

■ AUTHOR INFORMATION

Corresponding Authors

*E-mail: tsoh@stanford.edu (H.T.S.).
*E-mail: seungsoo@postech.ac.kr (S.S.O.).

ORCID

Hyongsok Tom Soh: 0000-0001-9443-857X

Notes

The authors declare no competing financial interest.

■ ACKNOWLEDGMENTS

This work was supported by NRF (National Research Foundation of Korea) Grant funded by the Korean Government (NRF-2017R1C1B3012050 and NRF-2018-Fostering Core Leaders of the Future Basic Science Program/Global Ph.D. Fellowship Program), and POSCO Green Science Program. H.T.S. is a Chan-Zuckerberg Biohub investigator.

■ REFERENCES

(1) Cui, Q.; Karplus, M. Allostery and cooperativity revisited. *Protein Sci.* **2008**, *17*, 1295−1307.
(2) Bhattacharya, S.; Bunick, C. G.; Chazin, W. J. Target selectivity in EF-hand calcium binding proteins. *Biochim. Biophys. Acta, Mol. Cell Res.* **2004**, *1742*, 69−79.
(3) Schatzmann, H. Dependence on calcium concentration and stoichiometry of the calcium pump in human red cells. *J. Physiol.* **1973**, *235*, 551−569.
(4) Jelkmann, W. Molecular biology of erythropoietin. *Intern. Med.* **2004**, *43*, 649−659.
(5) Carpenter, C. C.; Fischl, M. A.; Hammer, S. M.; Hirsch, M. S.; Jacobsen, D. M.; Katzenstein, D. A.; Montaner, J. S.; Richman, D. D.; Saag, M. S.; Schooley, R. T. Antiretroviral therapy for HIV infection in 1997: updated recommendations of the International AIDS Society—USA Panel. *JAMA, J. Am. Med. Assoc.* **1997**, *277*, 1962−1969.
(6) Bachmann, J.; Raue, A.; Schilling, M.; Böhm, M. E.; Kreutz, C.; Kaschek, D.; Busch, H.; Gretz, N.; Lehmann, W. D.; Timmer, J.; Klingmüller, U. Division of labor by dual feedback regulators controls JAK2/STAT5 signaling over broad ligand range. *Mol. Syst. Biol.* **2011**, *7*, 516.
(7) Lai, S. Y.; Childs, E. E.; Xi, S.; Coppelli, F. M.; Gooding, W. E.; Wells, A.; Ferris, R. L.; Grandis, J. R. Erythropoietin-mediated activation of JAK-STAT signaling contributes to cellular invasion in head and neck squamous cell carcinoma. *Oncogene* **2005**, *24*, 4442−4449.
(8) Koshland, D. E.; Goldbeter, A.; Stock, J. B. Amplification and adaptation in regulatory and sensory systems. *Science* **1982**, *217*, 220−225.
(9) Ferrell, J. E., Jr. Tripping the switch fantastic: How a protein kinase cascade can convert graded inputs into switch-like outputs. *Trends Biochem. Sci.* **1996**, *21*, 460−466.
(10) Yamazaki, T.; Kojima, K.; Sode, K. Extended-range glucose sensor employing engineered glucose dehydrogenases. *Anal. Chem.* **2000**, *72*, 4689−4693.
(11) VanEngelenburg, S. B.; Palmer, A. E. Fluorescent biosensors of protein function. *Curr. Opin. Chem. Biol.* **2008**, *12*, 60−65.
(12) Wang, Y.-C.; Han, J. Pre-binding dynamic range and sensitivity enhancement for immuno-sensors using nanofluidic preconcentrator. *Lab Chip* **2008**, *8*, 392−394.
(13) Ricci, F.; Vallée-Bélisle, A.; Simon, A. J.; Porchetta, A.; Plaxco, K. W. Using nature's "tricks" to rationally tune the binding properties of biomolecular receptors. *Acc. Chem. Res.* **2016**, *49*, 1884−1892.
(14) Porchetta, A.; Vallée-Bélisle, A.; Plaxco, K. W.; Ricci, F. Using distal-site mutations and allosteric inhibition to tune, extend, and narrow the useful dynamic range of aptamer-based sensors. *J. Am. Chem. Soc.* **2012**, *134*, 20601−20604.
(15) Porchetta, A.; Vallée-Bélisle, A.; Plaxco, K. W.; Ricci, F. Allosterically tunable, DNA-based switches triggered by heavy metals. *J. Am. Chem. Soc.* **2013**, *135*, 13238−13241.
(16) Mariottini, D.; Idili, A.; Nijenhuis, M. A.; de Greef, T. F.; Ricci, F. DNA-based nanodevices controlled by purely entropic linker domains. *J. Am. Chem. Soc.* **2018**, *140*, 14725−14734.
(17) Eisenberg, M. L.; Davies, B. J.; Cooperberg, M. R.; Cowan, J. E.; Carroll, P. R. Prognostic implications of an undetectable ultrasensitive prostate-specific antigen level after radical prostatectomy. *Eur. Urol.* **2010**, *57*, 622−630.
(18) Vallée-Bélisle, A.; Ricci, F.; Plaxco, K. W. Engineering biosensors with extended, narrowed, or arbitrarily edited dynamic range. *J. Am. Chem. Soc.* **2012**, *134*, 2876−2879.
(19) Oh, S. S.; Plakos, K.; Xiao, Y.; Eisenstein, M.; Soh, H. T. In vitro selection of shape-changing DNA nanostructures capable of binding-induced cargo release. *ACS Nano* **2013**, *7*, 9675−9683.
(20) Li, Y.; Geyer, R.; Sen, D. Recognition of anionic porphyrins by DNA aptamers. *Biochemistry* **1996**, *35*, 6911−6922.
(21) Travascio, P.; Li, Y.; Sen, D. DNA-enhanced peroxidase activity of a DNA aptamer-hemin complex. *Chem. Biol.* **1998**, *5*, 505−517.
(22) Kong, D.-M.; Xu, J.; Shen, H.-X. Positive effects of ATP on G-quadruplex-hemin DNAzyme-mediated reactions. *Anal. Chem.* **2010**, *82*, 6148−6153.
(23) Ding, N.; Yan, N.; Ren, C.; Chen, X. Colorimetric determination of melamine in dairy products by Fe_3O_4 magnetic nanoparticles− H_2O_2− ABTS detection system. *Anal. Chem.* **2010**, *82*, 5897−5899.
(24) Tien, M.; Svingen, B. A.; Aust, S. D. An investigation into the role of hydroxyl radical in xanthine oxidase-dependent lipid peroxidation. *Arch. Biochem. Biophys.* **1982**, *216*, 142−151.
(25) Braughler, J. M.; Duncan, L. A.; Chase, R. L. The involvement of iron in lipid peroxidation. Importance of ferric to ferrous ratios in initiation. *J. Biol. Chem.* **1986**, *261*, 10282−10289.
(26) Stefan, L.; Denat, F.; Monchaud, D. Insights into how nucleotide supplements enhance the peroxidase-mimicking DNAzyme activity of the G-quadruplex/hemin system. *Nucleic Acids Res.* **2012**, *40*, 8759−8772.
(27) Sazani, P. L.; Larralde, R.; Szostak, J. W. A small aptamer with strong and specific recognition of the triphosphate of ATP. *J. Am. Chem. Soc.* **2004**, *126*, 8370−8371.
(28) Vaish, N. K.; Larralde, R.; Fraley, A.; Szostak, J. W.; McLaughlin, L. W. A novel, modification-dependent ATP-binding aptamer selected from an RNA library incorporating a cationic functionality. *Biochemistry* **2003**, *42*, 8842−8851.
(29) Yu, P.; He, X.; Zhang, L.; Mao, L. Dual recognition unit strategy improves the specificity of the adenosine triphosphate (ATP)

DOI: 10.1021/acssensors.9b01503
ACS Sens. 2019, 4, 2802−2808

aptamer biosensor for cerebral ATP assay. *Anal. Chem.* **2015**, *87*, 1373−1380.
(30) Lungu, C.; Pinter, S.; Broche, J.; Rathert, P.; Jeltsch, A. Modular fluorescence complementation sensors for live cell detection of epigenetic signals at endogenous genomic sites. *Nat. Commun.* **2017**, *8*, No. 649.
(31) Kent, A. D.; Spiropulos, N. G.; Heemstra, J. M. General approach for engineering small-molecule-binding DNA split aptamers. *Anal. Chem.* **2013**, *85*, 9916−9923.
(32) Liu, X.; Shi, L.; Hua, X.; Huang, Y.; Su, S.; Fan, Q.; Wang, L.; Huang, W. Target-induced conjunction of split aptamer fragments and assembly with a water-soluble conjugated polymer for improved protein detection. *ACS Appl. Mater. Interfaces* **2014**, *6*, 3406−3412.
(33) Tang, J.; Shi, H.; He, X.; Lei, Y.; Guo, Q.; Wang, K.; Yan, L.; He, D. Tumor cell-specific split aptamers: target-driven and temperature-controlled self-assembly on the living cell surface. *Chem. Commun.* **2016**, *52*, 1482−1485.
(34) Sharma, A. K.; Heemstra, J. M. Small-molecule-dependent split aptamer ligation. *J. Am. Chem. Soc.* **2011**, *133*, 12426−12429.
(35) Yu, T.; Zhou, W.; Liu, J. Ultrasensitive DNAzyme-based Ca^{2+} detection boosted by ethanol and a solvent-compatible scaffold for aptazyme design. *ChemBioChem* **2018**, *19*, 31−36.
(36) Cochrane, J. C.; Lipchock, S. V.; Strobel, S. A. Structural investigation of the GlmS ribozyme bound to its catalytic cofactor. *Chem. Biol.* **2007**, *14*, 97−105.
(37) Sun, Y.; Ma, R.; Wang, S.; Li, G.; Sheng, Y.; Rui, H.; Zhang, J.; Xu, J.; Jiang, D. New cofactors and inhibitors for a DNA-cleaving DNAzyme: superoxide anion and hydrogen peroxide mediated an oxidative cleavage process. *Sci. Rep.* **2017**, *7*, No. 378.
(38) Roth, A.; Breaker, R. R. An amino acid as a cofactor for a catalytic polynucleotide. *Proc. Natl. Acad. Sci. U.S.A.* **1998**, *95*, 6027−6031.
(39) Cho, M.; Oh, S. S.; Nie, J.; Stewart, R.; Eisenstein, M.; Chambers, J.; Marth, J. D.; Walker, F.; Thomson, J. A.; Soh, H. T. Quantitative selection and parallel characterization of aptamers. *Proc. Natl. Acad. Sci. U.S.A.* **2013**, *110*, 18460−18465.
(40) Oh, S. S.; Ahmad, K. M.; Cho, M.; Kim, S.; Xiao, Y.; Soh, H. T. Improving aptamer selection efficiency through volume dilution, magnetic concentration, and continuous washing in microfluidic channels. *Anal. Chem.* **2011**, *83*, 6883−6889.
(41) Gotrik, M. R.; Feagin, T. A.; Csordas, A. T.; Nakamoto, M. A.; Soh, H. T. Advancements in aptamer discovery technologies. *Acc. Chem. Res.* **2016**, *49*, 1903−1910.
(42) Qu, H.; Csordas, A. T.; Wang, J.; Oh, S. S.; Eisenstein, M. S.; Soh, H. T. Rapid and label-free strategy to isolate aptamers for metal ions. *ACS Nano* **2016**, *10*, 7558−7565.
(43) Silverman, S. K. Nucleic Acid Enzymes (Ribozymes and Deoxyribozymes): In Vitro Selection and Application. In *Encyclopedia of Chemical Biology*, 1st ed.; Wiley: New York, 2007; pp 1−17.
(44) Walter, J.-G.; Stahl, F. Aptazymes: Expanding the Specificity of Natural Catalytic Nucleic Acids by Application of In Vitro Selected Oligonucleotides. In *Advances in Biochemical Engineering/Biotechnology*; Springer: Berlin, 2019.

DOI: 10.1021/acssensors.9b01503
ACS Sens. 2019, 4, 2802−2808